Modeling Iridium-Based Trilayer and Bilayer Transition-Edge Sensors

Gensheng Wang, Jeffrey Beeman, Clarence L. Chang, Junjia Ding, A. Drobizhev, B. K. Fujikawa, K. Han, S. Han,
R. Hennings-Yeomans, Goran Karapetrov, Yury G. Kolomensky, Valentyn Novosad, T. O'Donnell, J. L. Ouellet,
John Pearson, B. Sheff, V. Singh, S. Wagaarachchi, J. G. Wallig, and Volodymyr G. Yefremenko

Abstract—We report a model that can be used to calculate superconducting transition temperature of a transition-edge sensor (TES), which is either a normal metal–superconductor–normal metal trilayer or a normal metal–superconductor bilayer. The model allows the T_C estimation of a trilayer when the normal metals at the bottom and at the top are different. Furthermore, the model includes the spin flip time of the normal metals. We use the T_C calculations from this model for selected Ir-based trilayers and bilayers to help understand potential designs of low T_C TESs. A Au/Ir/Au trilayer can have a low T_C because the superconducting order parameter is reduced with normal metals at both sides. On the other hand, an Ir/Pt bilayer can have a low T_C because the much larger electron density of states of Pt reduces the superconducting order parameter more effectively. Moreover, the spin flip scattering of paramagnetic Pt also contributes to the T_C reduction.

Index Terms—Superconductivity, proximity effect, transition-edge sensor, Usadel equations.

G. Wang and V. G. Yefremenko are with the High Energy Physics Division, Argonne National Laboratory, Lemont, IL 60439 USA (e-mail: gwang@anl.gov; yefremenko@anl.gov).

J. Beeman is with the Materials Science Division, Lawrence Berkeley National Laboratory, Berkeley, CA 94720 USA (e-mail: JWBeeman@lbl.gov).

C. L. Chang is with the High Energy Physics Division, Argonne National Laboratory, Lemont, IL 60439 USA, and also with the Kavli Institute for Cosmological Physics and Department of Astronomy and Astrophysics, University of Chicago, Chicago, IL 60637 USA (e-mail: clchang@kicp.uchicago.edu).

J. Ding, V. Novosad, and J. Pearson are with the Materials Science Division, Argonne National Laboratory, Lemont, IL 60439 USA (e-mail: dingj@anl.gov; novosad@anl.gov; pearson@anl.gov).

A. Drobizhev, R. Hennings-Yeomans, T. O'Donnell, and S. Wagaarachchi are with the Department of Physics, University of California, Berkeley, CA 94720 USA, and also with the Nuclear Science Division, Lawrence Berkeley National Laboratory, Berkeley, CA 94720 USA (e-mail: lyoshadrobizhev@berkeley.edu; hennings@berkeley.edu; tdonnell@berkeley.edu; sachi@berkeley.edu).

B. K. Fujikawa is with the Nuclear Science Division, Lawrence Berkeley National Laboratory, Berkeley, CA 94720 USA (e-mail: bkfujikawa@lbl.gov).

K. Han is with the Department of Physics, Yale University, New Haven, CT 06520 USA (e-mail: ke.han@yale.edu).

S. Han, B. Sheff, and V. Singh are with the Department of Physics, University of California, Berkeley, CA 94720 USA (e-mail: sojinsmilev2@berkeley.edu; ben1sheff@berkeley.edu; singhv@berkeley.edu).

G. Karapetrov is with the Physics Department, Drexel University, Philadelphia, PA 19104 USA (e-mail: goran@drexel.edu).

Y. G. Kolomensky is with the Department of Physics, University of California, Berkeley, CA 94720 USA, and also with the Nuclear Science Division and Physics Division, Lawrence Berkeley National Laboratory, Berkeley, CA 94720 USA (e-mail: YGKolomensky@lbl.gov).

J. L. Ouellet is with the Department of Physics, University of California, Berkeley, CA 94720 USA, and also with the Massachusetts Institute of Technology, Cambridge, MA 02139 USA (e-mail: ouelletj@mit.edu).

J. G. Wallig is with the Engineering Division, Lawrence Berkeley National Laboratory, Berkeley, CA 94720 USA (e-mail: jgwallig@lbl.gov).

Color versions of one or more of the figures in this paper are available online at http://ieeexplore.ieee.org.

Digital Object Identifier 10.1109/TASC.2016.2646373

I. INTRODUCTION

IN LOW-BACKGROUND experiments exploring fundamental physics, such as cryogenic Neutrino-less Double Beta Decay (NLDBD) searches [1], [2] and Dark Matter (DM) particle searches [3], [4], the TES can be an ideal thermometer. First, its large bandwidth can help capture a signal pulse shape to identify the particle's type and to provide event position information. Second, low impedance TES can be multiplexed to tens of thousands of channels, which may improve scaling of the experimental mass. On the other hand, reproducible fabrication of a large number of TES with required low T_C is not trivial. We have been making Ir-based bilayer and trilayer low T_C TESs using the proximity effect. Previously it was found that to make an Ir/Au bilayer TES with $T_C < 30$ mK, the substrate needs to be heated up to 500 °C during the sputtering deposition of the Ir film [5]. Recently it was observed that low T_C TESs can be made with substrates at room temperature: a Au(200 nm)/Ir(100 nm)/Au(200 nm) trilayer can have a T_C close to 20 mK, and an Ir(100 nm)/Pt(80 nm) bilayer can have a similarly low T_C [5]. This work is motivated to understand the T_C of an Ir-based trilayer or bilayer.

The proximity effect, with which transition temperature of a superconductor can be reduced with a normal metal, is historically understood as a boundary effect [6], [7]. But the theory cannot match data without adding in an artificial factor in the T_C prediction equations [8]. A modern realization is that the proximity effect can be understood with the Usadel theory [9] by introducing an interface resistance and by applying proper boundary conditions [10], [11].

In this paper, we solve the Usadel equations, which are parameterized with a pairing angle in the microscopic superconductivity theory. A comprehensive description of the Usadel equations and their boundary conditions can be found in references [12]–[14]. In Section II, by solving the Usadel equations with the thin films approximation, we extend the T_C calculation
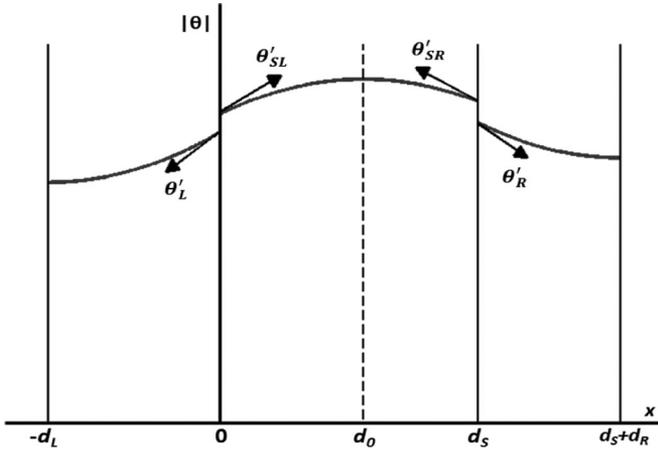
Fig. 1.   The amplitude of the superconducting pairing parameter θ vs position x for a NSN trilayer. The superconductor is from 0 to d_S. There are two metals. One is from $-d_L$ to 0 on the left, another is from d_S to $d_S + d_R$ on the right. The amplitude of θ_S in the superconductor peaks at d_0, where $\theta_S' = 0$.

method of a bilayer in [14] to that of a NSN trilayer and include the effects due to spin flip scattering in the normal metals. We will estimate transition temperatures of an Ir/Au bilayer, an Ir/Pt bilayer, a Au/Ir/Au trilayer, and a Pt/Ir/Au trilayer in Section III. We conclude in Section IV.

II. Transition Temperature of a Trilayer or a Bilayer

A trilayer consists of a normal metal with a thickness of d_L on the left, a superconductor with a thickness of d_S and a transition temperature of T_{CS} in the middle, and a normal metal with a thickness of d_R on the right. See Fig. 1. In the dirty limit (electron mean free path is less than coherence length), the properties of a superconductor in contact with a metal can be described with the Usadel equations [10]–[14]. In microscopic theory, the superconducting state is described by a function $\theta(x, E)$ called the pairing angle, where x is a position coordinate and E is energy. The variable θ is complex and ranges in magnitude from 0 to $\pi/2$. $\theta = 0$ corresponds to the normal state. The Usadel equations used to solve for $\theta(x, E)$ are

$$\frac{\hbar D_S}{2} \frac{\partial^2 \theta_S}{\partial x^2} + iE \sin \theta_S - \left[\frac{\hbar}{\tau} + \frac{\hbar D_S}{2} \left(\frac{\partial \varphi}{\partial x} + \frac{2e}{\hbar} A_x \right)^2 \right]$$

$$\times \cos \theta_S \sin \theta_S + \Delta(x) \cos \theta_S = 0 , \qquad (1)$$

and

$$\Delta(x) = N_S V_{\text{eff}} \int_0^{\hbar \omega_D} dE \tanh(E/2k_B T) \, \text{Im} \left[\sin \theta_S \right] , \quad (2)$$

where $D_S = \sigma_S / N_S e^2$ is the diffusivity of the superconductor, N_S is the density of states at the Fermi energy, σ_S is the normal state conductivity, and e is the electron charge. φ is the usual superconducting phase parameter. A_x is the vector potential. τ is the electron spin-flip time. $\Delta(x)$ is the superconducting order parameter. V_{eff} is the BCS-like interaction potential. $\hbar$ is the reduced Plank constant. ω_D is the Debye frequency. k_B is the Boltzmann constant. And T is the temperature.

In the equation (1), the spin-flip scattering, current ($\partial \varphi / \partial x$ term) and magnetic field contribute to pair breaking [14]. With a small current and in absence of an external magnetic field, only the spin-flip time in paramagnetic metals [15]–[17] needs to be kept in a proximity effect analysis [18]–[20]. Near the T_C of a trilayer, the pairing angle satisfies $|\theta| \ll 1$ in all three layers. It's assumed that each film is thinner than its coherence length. Therefore, the pairing angle θ is approximately the same (almost constant) in the film. In the following calculations, we only include the dependence of θ on x up to quadrature term ($\partial \theta^2 / \partial x^2$ is constant) [14]. In the superconductor ($0 < x < d_S$ in Fig. 1), it's assumed that the electron has no spin-flip scattering. The equation (1) can then be linearized as

$$\frac{\hbar D_S}{2} \frac{\partial^2 \theta_S}{\partial x^2} + iE \theta_S + \Delta(x) = 0 . \qquad (3)$$

For the normal metals ($-d_L < x < 0$ and $d_S < x < d_S + d_R$ in Fig. 1), $V_{\text{eff}} = 0$. By linearizing the equation (1), the paring angle parameter θ_L or θ_R satisfies

$$\frac{\hbar D_{L,R}}{2} \frac{\partial^2 \theta_{L,R}}{\partial x^2} + iE \theta_{L,R} - \frac{\hbar}{\tau_{L,R}} \theta_{L,R} = 0 , \qquad (4)$$

where $D_L = \sigma_L / N_L e^2$ and $D_R = \sigma_R / N_R e^2$ are the diffusivities of the normal metals on the left and on the right respectively, N_L and N_R are the density of states at the Fermi energies respectively, and σ_L and σ_R are the normal state conductivities respectively. Electron spin-flip times τ_L and τ_R are kept for potential paramagnetic property in normal metals [15]–[20].

The equations (3) and (4) are complemented with boundary conditions [10]–[14]. There are two kinds of boundaries. The first kind of boundary faces a vacuum or a dielectric. There is no current flowing out. Therefore, $\partial \theta_L / \partial x = 0$ at $x = -d_L$ and $\partial \theta_R / \partial x = 0$ at $x = d_S + d_R$ in Fig. 1.

The second kind of boundary connects two metals together. The current across the interface is conserved. Therefore, at the interface $x = 0$,

$$\sigma_S \frac{\partial \theta_{SL}}{\partial x} = \sigma_L \frac{\partial \theta_L}{\partial x} = g_L (\theta_{SL} - \theta_L) , \qquad (5)$$

where $g_L = G_L / A$. A is the area of the interface. $G_L = 2t_L N_{Ch} G_K$ is the interface conductance between the normal metal on the left and the superconductor, where t_L is a free parameter describing electron transmission coefficient across the interface, $N_{Ch} = A / (\lambda_{\text{f}}/2)^2$ is the number of conductance channels, and λ_{f} is the Fermi wavelength in the metal or the superconductor that has fewer conductance channels, and $G_K = e^2 / h$ is the conductance quantum. Similarly, at the interface where $x = d_S$,

$$\sigma_S \frac{\partial \theta_{SR}}{\partial x} = \sigma_R \frac{\partial \theta_R}{\partial x} = g_R (\theta_R - \theta_{SR}) , \qquad (6)$$

where $g_R = G_R / A$. $G_R = 2t_R N_{Ch} G_K$ is the interface conductance between the normal metal on the right and the superconductor, where t_R is a free parameter describing electron transmission coefficient across the interface.

By applying the boundary condition $\partial \theta_L / \partial x = 0$ at $x = -d_L$, it's found that $\partial \theta_L / \partial x = d_L (\partial \theta_L^2 / \partial x^2)$ at $x = 0$. By applying the boundary condition $\partial \theta_R / \partial x = 0$

at $x = d_S + d_R$, it's found that $\partial\theta_R/\partial x = -d_R(\partial\theta_R^2/\partial x^2)$ at $x = d_S$. By utilizing the equation (4), the pairing angle θ_L at $x = 0$ or the pairing angle θ_R at $x = d_S$ satisfies

$$\frac{\partial\theta_{L,R}}{\partial x} = \mp\left(iE - \frac{\hbar}{\tau_{L,R}}\right)\theta_{L,R}\frac{2d_{L,R}}{\hbar D_{L,R}} , \quad (7)$$

where the "$-$" sign in the equation is for θ_L at $x = 0$ and the "$+$" sign is for θ_R at $x = d_S$.

In the superconductor, the calculation is simplified with the approximation that the small θ_S near the T_C only depends on x up to the quadrature term. The amplitude of θ_S peaks at d_0, therefore, $\partial\theta_S/\partial x = 0$ at $x = d_0$. It's straightforward to find that $\partial\theta_{SL}/\partial x = -d_0(\partial\theta_S^2/\partial x^2)$ at $x = 0$ and $\partial\theta_{SR}/\partial x = (d_S - d_0)(\partial\theta_S^2/\partial x^2)$ at $x = d_S$. By utilizing the equation (3), the pairing angle θ_{SL} at $x = 0$ or the pairing angle θ_{SR} at $x = d_S$ satisfies

$$\frac{\partial\theta_{SL,SR}}{\partial x} = \pm(iE\theta_S + \Delta)\frac{2d_X}{\hbar D_S} , \quad (8)$$

where the "$+$" sign with $d_X = d_0$ in the equation is for θ_{SL} at $x = 0$, the "$-$" sign with $d_X = d_S - d_0$ is for θ_{SR} at $x = d_S$. Note that the same θ_S is used in the equation (8) for both θ_{SL} and θ_{SR}, which means the θ_S is approximately constant in the thin superconducting film. d_0 and θ_S can be found by solving equations (5)–(8). Both d_0 and θ_S depend on energy E.

An electron coherence length can be defined at a low frequency approximation $E = i\omega$, where $\omega = \pi k_B T$ is Matsuburu frequency at the lowest order [6], [7]. In the equation (7), the coherence length of the normal metal on the left or on the right in Fig. 1 is $\xi_{L,R} = \sqrt{\hbar D_{L,R}/2\pi k_B T(1 + \hbar/\pi k_B T\tau_{L,R})}$. In the equation (8), the coherence length of the superconductor in the middle without spin-flip scattering is $\xi_S = \sqrt{\hbar D_S/2\pi k_B T}$. The coherence length aids in understanding the material characteristics and calculation results in next section.

To continue the modeling without a low frequency approximation, θ_S can be written as

$$\theta_S = \frac{i\Delta}{E}(1 - (f_A + if_B)) , \quad (9)$$

with

$$f_A + if_B = \frac{1}{1 - iEd_S f_1 f_2/(f_1 + f_2)} , \quad (10)$$

where f_A and f_B are real numbers. The functions f_1 and f_2 are

$$f_{1,2} = a_{L,R}N_S - \frac{1}{iE - \hbar/\tau_{L,R}}\frac{N_S}{N_{L,R}}\frac{1}{d_{L,R}} , \quad (11)$$

where $a_L = 4\pi G_K/g_L$ and $a_R = 4\pi G_K/g_R$.

Taking the imaginary part of θ_S in the equation (9) and inserting into the order parameter equation (2), it's found that

$$\frac{1}{N_S V_{\text{eff}}} = \int_0^{\hbar\omega_D}\frac{dE}{E}(1 - f_A)\tanh\left(\frac{E}{2k_B T_C}\right) . \quad (12)$$

The first term in the equation (12) is the electron-phonon interaction in the superconductor film, which defines T_{CS}. The second term is a modification of the electron-phonon interaction due to the normal metal and superconductor contact. So, the T_C

Parameter	Ir	Au	Pt
Electron phonon coupling constant λ [a, b]	0.34	0.17	0.60
Electronic specific heat γ in JK^{-2} m^{-3} [a, b]	3.70×10^2	7.15×10^1	7.29×10^2
Fermi wavelength λ_f in nm [c]	0.536	0.518	0.609
Resistivity at 300 K ρ_{300} in 10^{-8} Ω m [d, e]	5.2	2.2	10.9
Debye temperature θ_D in Kelvin [f]	420	165	240
Electron coherence length ξ in nm [g]	379	1355	194

[a]Ref. [21]; [b]Ref. [22]; [c]Ref. [23]; [d]Ref. [24]; [e]Ref. [25]; [f]Ref. [26].
[g]$\xi = \sqrt{\hbar D/2\pi k_B T} = \sqrt{\hbar\pi k_B 6e^2\gamma\rho T}$ [27], where $T = 30$ mK.

of the NSN trilayer can be found with

$$\ln\left(\frac{T_C}{T_{CS}}\right) = -\int_0^{\hbar\omega_D}\frac{dE}{E}(f_A)\tanh\left(\frac{E}{2k_B T_C}\right) , \quad (13)$$

where f_A is calculated using the equations (10)-(11). The T_C can be calculated with an iterative method.

For a NS bilayer consisting of a normal metal where $-d_L < x < 0$ and a superconductor where $0 < x < d_0$ in Fig. 1, we solve the equation (5), the equation (7) with the "$-$" sign, and the equation (8) the "$+$" sign for θ_S in the superconductor. We can write θ_S in the form of equation (9) with

$$f_A = \frac{f_1}{1 + f_2^2} , \quad (14)$$

where

$$f_1 = \frac{1 + \frac{\hbar^2}{(E\tau_L)^2}}{1 + \frac{\hbar^2}{(E\tau_L)^2} + \frac{d_0 N_S}{d_L N_L}} , \quad (15)$$

and

$$f_2 = \frac{\left(1 + \frac{\hbar^2}{(E\tau_L)^2}\right)d_0 N_S E a_L + \frac{\hbar}{E\tau_L}\frac{d_0 N_S}{d_L N_L}}{1 + \frac{\hbar^2}{(E\tau_L)^2} + \frac{d_0 N_S}{d_L N_L}} . \quad (16)$$

So, the T_C of a NS bilayer can be estimated using the equation (13), where f_A is calculated with the equations (14)–(16).

The calculations above are for the normal metals with a large electron spin flip rate $1/\tau_L$. At a small spin flip rate, $\hbar/E\tau_L \ll 1$, it can be verified that the equation (13) can be simplified to the equation (7) in [14], which is for the T_C calculation of a nonmagnetic metal superconductor bilayer.

III. T_C CALCULATION OF NSN TRILAYERS AND NS BILAYERS

We calculate the transition temperatures of Ir/Au and Ir/Pt bilayers using the equations (13) and (14)-(16), and that of Au/Ir/Au and Pt/Ir/Au trilayers using the equations (13) and (10)–(11). The input physical parameters from literature [21]–[26] are listed in Table I. The electron coherence length is also estimated in the table. We use electron specific heat density of states, $N_{N,S} = 3\gamma_{N,S}/\pi^2 k_B^2(1 + \lambda_{N,S})$ [26] for the normal metals N and the superconductor S. In addition, we assume the residual resistance ratio $RRR = 3$ for all films. The electron conductivity $\sigma = 1/\rho$ and $\rho = \rho_{300}/RRR$.
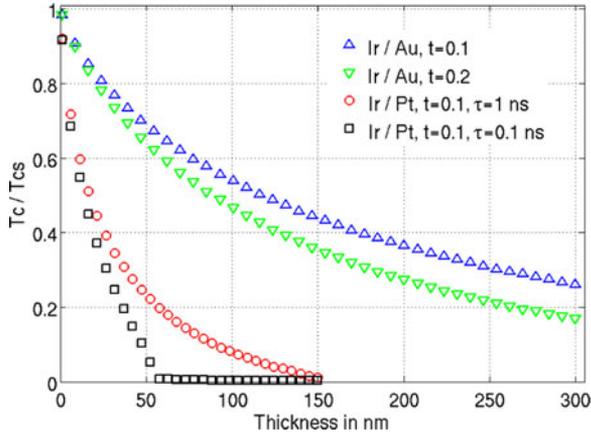
Fig. 2. The T_C of Ir/Au and Ir/Pt bilayers normalized to T_{CS}. Ir film is 100 nm thick for all the four curves. t in the legend is for the electron transmission coefficient across the interface. τ is for electron spin flip time in Pt.
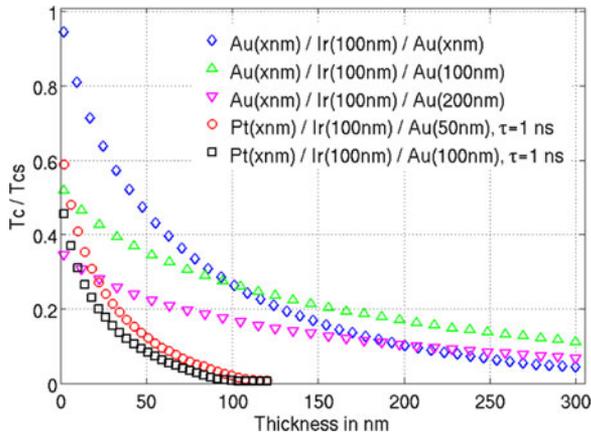

Fig. 3. The T_C of Au/Ir/Au and Pt/Ir/Au trilayers normalized to T_{CS}. The electron transmission coefficient across the interface is $t = 0.1$ for all the five curves. τ is for electron spin flip time in Pt.

Fig. 2 shows the transition temperatures normalized to the bare superconducting film's T_{CS} for Ir/Au and Ir/Pt bilayers. The blue triangles and the green inverse triangles demonstrate that the T_C of a NS bilayer is lower when the electron transmission coefficient across the interface is larger. The result is consistent with other studies [13], [28]–[30]. It is also observed that a Pt film suppresses the T_C of an Ir film more strongly than a Au film does. The observation is related to both the large specific heat coefficient and the strong paramagnetic property of Pt [31], [32]. First, the one order of magnitude larger electron density of states (which is calculated with λ and γ data in Table I) in Pt than in Au enhances the T_C suppression. Secondly, the paramagnetic effect in Pt, whose strength is characterized with a spin-flip time, suppresses cooper pairs. Note that a spin-flip time $\tau = 0.08$ ns corresponds to $\hbar/\pi k_B T\tau \approx 1$ at $T = 30$ mK. A spin-flip time τ larger than 1 ns, which corresponds to $\hbar/\pi k_B T\tau \ll 1$, has a negligible impact to the T_C of an Ir/Pt bilayer.

Fig. 3 shows the transition temperatures normalized to the bare superconducting film's T_{CS} for Au/Ir/Au and Pt/Ir/Au

trilayers. By comparing the blue diamonds in Fig. 3 and the blue triangles in Fig. 2, it's realized that the Ir film's T_C is suppressed more effectively when Au films are used at both sides of an Ir film. This strategy in making a low T_C TES is important when an Ir film's T_C is high. For example, thin Ir films sputtered at room temperature can have a fairly high T_C [33], [34], but there are advantages in making a TES without substrate heating. By comparing the T_C data of Ir/Au and Ir/Pt bilayers in Fig. 2 as well as the resistivity and specific heat coefficient data in Table I, it may make sense to use a Pt/Ir/Au trilayer. A Pt film, which has a high resistivity and a large specific heat ($c = \gamma T$ for a metal. See Table I for γ data), can be used to control the T_C of a TES at the bottom. A Au film, which has low resistivity and a small specific heat can be used as a passivation layer on the top. As such, while the low T_C of a TES is well defined, there is an additional adjustability in its resistance or heat capacity. The transition temperatures as a function of Pt film thickness for two Pt/Ir/Au configurations are shown in Fig. 3 as the red circles and black squares.

IV. CONCLUSION

By solving the microscopic Usadel equations with proper boundary conditions, the T_C calculation methods of an NSN trilayer and a NS bilayer are developed. Material properties such as electron density of states, electron transmission efficiency across the interface of metals and electron spin-flip time of normal metals are included in the methods. The transition temperatures of Ir-based bilayers and trilayers are calculated with physical parameters available from the literature. There are several options to make an Ir-based low T_C TES without substrate heating. They can be an Ir/Pt bilayer, a Pt/Ir/Au trilayer and a Au/Ir/Au trilayer respectively.

REFERENCES

[1] K. Alfonso *et al.*, "Search for neutrinoless double-beta decay of ^{130}Te with CUORE-0," *Phys. Rev. Lett.*, vol. 115, 2015, Art. no. 102502.
[2] G. Wang *et al.*, "R&D towards CUPID (CUORE Upgrade with Particle Identification)," 2015. [Online]. Available: http://arxiv.org/pdf/1504.03612v1.pdf
[3] Z. Ahmed *et al.*, "Search for weakly interacting massive particles with the first five-tower data from the cryogenic dark matter search at the Soudan underground laboratory," *Phys. Rev. Lett.*, vol. 102, 2009, Art. no. 011301.
[4] G. Angloher *et al.*, "Results from 730 kg days of the CRESST-II dark matter search," *Eur. Phys. J. C*, vol. 72, 2012, Art. no. 1971.
[5] R. Hennings-Yeomans *et al.*, "Development of low-Tc transition edge sensors for neutrino-less double beta decay," in *Proc. Appl. Supercond. Conf.*, Denver, CO, USA, Sep. 4–9, 2016, Paper 1EOr3C-01.
[6] N. R. Werthamer, "Theory of the superconducting transition temperature and energy gap function of superposed metal films," *Phys. Rev.*, vol. 132, no. 6, pp. 2440–2445, 1963.
[7] P. G. de Gennes, "Boundary effects in superconductors," *Rev. Mod. Phys.*, vol. 36, pp. 225–237, 1964.
[8] U. Nagel *et al.*, "Proximity effect in iridium-gold bilayers," *J. Appl. Phys.*, vol. 110, 1994, Art. no. 063919.
[9] K. D. Usadel "Generalized diffusion equation for superconducting alloys," *Phys. Rev. Lett.*, vol. 25, pp. 507–509, 1970.
[10] M. Yu. Kupriyanov and V. F. Lukichev, "Influence of boundary transparency on the critical current of "dirty" SS'S structures," *Sov. Phys. JETP*, vol. 67, pp. 1163–1168, 1988.
[11] A. A. Golubov, M. Y. Kupriyanov, and E. Il'ichev, "The current-phase relation in Josephson junctions," *Rev. Mod. Phys.*, vol. 76, pp. 411–469, 2004.

[12] S. Gueron, H. Pothier, N. O. Birge, D. Esteve, and M. H. Devoret, "Superconducting proximity effect probed on a mesoscopic length scale," *Phys. Rev. Lett.*, vol. 77, no. 14, pp. 3025–3028, 1996.

[13] Y. V. Fominov and M. V. Feigel'man, "Superconductive properties of thin dirty superconductor-normal metal bilayers," *Phys. Rev. B*, vol. 63, 2001, Art. no. 094518.

[14] J. M. Martinis, G. C. Hilton, K. D. Irwin, and D. A. Wollman, "Calculation of T_C in a normal-superconductor bilayer using the microscopic-based Usadel theory," *Nuclear Instrum. Methods Phys. Res., Section A*, vol. 444, no. 1/2, pp. 23–27, 2000.

[15] D. Katayama, A. Sumiyama, and Y. Oda, "Proximity-induced superconductivity in platinum metals," *Phys. Rev. B*, vol. 68, 2003, Art. no. 132502.

[16] T. Herrmannsdörfer, S. Rehmann, W. Wendler, and F. Pobell, "Magnetic properties of highly diluted PdFex and PtFex alloys. Part I. Magnetization at Kelvin temperatures," *J. Low Temp. Phys.* vol. 104, no. 1/2, pp. 49–65, 1996.

[17] T. Herrmannsdörfer, S. Rehmann, and F. Pobell, "Magnetic properties of highly diluted PdFex and PtFex alloys. Part II. Susceptibility at Micro- and Milli-Kelvin temperature," *J. Low Temp. Phys.*, vol. 104, no. 1/2, pp. 67–94, 1996.

[18] T. Kontos, M. Aprili, J. Lesueur, X. Grison, and L. Dumoulin, "Superconducting proximity effect at the paramagnetic-ferromagnatic transition," *Phys. Rev. Lett.*, vol. 93, 2004, Art. no. 137001.

[19] O. Entin-Wohlman, "Proximity effects between superconducting and magnetic films," *Phys. Rev. B*, vol. 12, no. 11, pp. 4860–4866, 1975.

[20] J. J. Hauser, H. C. Theuerer, and N. R. Werthamer, "Proximity effects between superconducting and magnetic films," *Phys. Rev.*, vol. 142, no. 1, pp. 118–126, 1966.

[21] W. John, V. V. Nemosilkalenko, V. N. Antonov, and VL. N. Antonov, "Electron phonon interaction in transition metals, results of relativistic APW band structure calculations," *Phys. Status Solidi (b)*, vol. 121, pp. 233–239, 1984.

[22] Z. Lin, L. V. Zhigilei, and V. Celli, "Electron-phonon coupling and electron heat capacity of metals under conditions of strong electron-phonon nonequilibrium," *Phys. Rev. B*, vol. 77, 2008, Art. no. 075133.

[23] C. Reale, "Conductivity data for the transition metals derived from considerations on the charge transport in thin films," *J. Phys. F*, vol. 4, pp. 2218–2222, 1974.

[24] D. Gall, "Electron mean free path in elemental metals," *J. Appl. Phys.*, vol. 119, 2016, Art. no. 085101.

[25] J. W. Arblaster, "Selected electrical resistivity values for platinum group of metals part I: Palladium and platinum," *Johnson Matthey Technol. Rev.*, vol. 59, pp. 174–181, 2015.

[26] C. Kittel, *Introduction to Solid State Physics*, 7th ed. Hoboken, NJ, USA: Wiley, 1996.

[27] J. J. Hauser, N. R. Werthamer, and H. C. Theuerer, "Superconductivity in Cu + Pt by means of superimposed films with lead," *Phys. Rev. A*, vol. 136, no. 3A, pp. A637–A641, 1964.

[28] A. A. Golubov, "Proximity effect in dirty N/S multilayers," *Proc. SPIE*, vol. 2157, pp. 353–362, 1994.

[29] C. Cirillo, S. L. Prischepa, M. Salvato, and C. Attanasiob, "Interface transparency of Nb/Pd layered systems," *Eur. Phys. J. B*, vol. 38, pp. 59–64, 2004.

[30] R. Boucher, T. May, T. Wagner, V. Zakosarenko, S. Anders, and H. G. Mayer, "Structural and electrical properties of AuPd/Mo bi-layer films for transition edge sensors," *Supercond. Sci. Technol.*, vol. 19, pp. 138–142, 2006.

[31] K. Andres and M. A. Jensen, "Superconductivity, susceptibility, and specific heat in the noble transition elements and alloys. I. Experimental results," *Phys. Rev.*, vol. 165, no. 2, pp. 533, 1968.

[32] M. A. Jensen and K. Andres, "Superconductivity, susceptibility and specific heat in noble transition elements and alloys. 2. Comparison with theory," *Phys. Rev.*, vol. 165, no. 2, pp. 545–555, 1968.

[33] D. Fukuda, H. Takahashi, M. Ohno, and M. Nakazawa, "Ir TES for X-ray microcalorimeters," *Nucl. Instrum. Methods A*, vol. 444, pp. 241–244, 2000.

[34] M. Galeazzi, D. Bogorin, R. Molina, M. Ribiro Gomes, and T. Saab, "Detector development for the MARE neutrino experiment," *AIP Conf. Proc.*, vol. 1185, pp. 558–561, 2009.